Check for updates

Environmental sustainability of cellulose-supported solid ionic liquids for CO_2 capture†

Pelayo García-Gutiérrez,[a] Rosa M. Cuéllar-Franca,[a] Dan Reed,[b] George Dowson,[b,c] Peter Styring[b] and Adisa Azapagic [ID] *[a]

Solid ionic liquids (SoILs) with cellulose as a support have been demonstrated recently to be effective and low-cost sorbents for CO_2 capture. However, at present it is not clear whether they remove more CO_2 than is released in the rest of the life cycle, including their manufacture, regeneration and disposal. It is also unknown what other impacts they may have over the whole life cycle while attempting to mitigate climate change. Therefore, this study evaluates for the first time the life cycle environmental sustainability of cellulose-supported SoILs in comparison with unsupported SoILs and some other sorbents. Four SoILs are assessed for 11 life cycle impacts, including global warming potential (GWP), with and without the cellulose support: methyltrioctyl ammonium acetate ([N_{1888}][Ac]), tetraethyl ammonium acetate ([N_{4444}][Ac]), tetra-octylammonium bromide ([N_{8888}]Br) and 1-butyl-4-methylimidazolium bromide ([Bmim]Br). They are compared with one of the ILs in the liquid state (trihexyltetradecylphosphonium 1,2,4-triazolide ([P_{66614}][124Triz])) and with three conventional sorbents: monoethanolamine (MEA), zeolite powder and activated carbon. The results show that SoILs with cellulose loading in the range of 70%–80 wt% have better environmental performance per unit mass of CO_2 captured than the unsupported SoILs. The net removal of CO_2 eq. over the life cycle ranges from 20% for pure [Bmim]Br to 83% for [N_{1888}][Ac] with 75% cellulose and for [N_{4444}][Ac] with both 75% and 80% loadings. However, pure [N_{8888}]Br generates three times more CO_2 eq. over the life cycle than it removes. Among the SoILs, [N_{4444}][Ac] with 80% cellulose has the lowest life cycle impacts for eight out of 11 categories. When compared to the conventional sorbents, it has significantly higher impacts, including GWP. However, it is more sustainable than [P_{66614}][124Triz]. The results of this study can be used to target the hotspots and improve the environmental performance of cellulose-supported SoILs through sustainable design.

1 Introduction

Reducing greenhouse gas (GHG) emissions and improving the security of energy supply within the context of an ever-growing energy demand have become major global challenges. Carbon capture and storage (CCS) along with carbon capture and utilisation (CCU) are seen as potentially viable technological options that can contribute towards reducing CO_2 emissions.[1–3] However, their successful commercial implementation depends, among other factors, on the efficiency of

CO_2 capture and its net removal on a life cycle basis, which can in turn influence significantly their economic and environmental sustainability. Currently, the most advanced large-scale CO_2 capture technologies rely on amine-based solutions, such as monoethanolamine (MEA).[4–6] This is due to a range of advantages they provide, including high absorption capacity and high selectivity towards other gases.[7] However, they are liable to evaporation losses, corrosive at elevated temperatures and their regeneration is energy intensive owing to the stability of the carbamate salt formed in the reaction between CO_2 and MEA.[6,8,9]

Over the last few years, alternative sorbents have been suggested for CO_2 capture.[10] Among these, ionic liquids (ILs), which are defined as organic salts with melting points below 120–140 °C,[11] have shown high CO_2 affinity and hence have attracted significant attention.[10,12] In contrast to amine-based solvents, ILs have negligible vapour pressure and low corrosivity.[10,13] In addition, many of them are chemically stable at elevated temperatures.[14] Furthermore, the large number of possible combinations of cations and anions in the

[a]*Sustainable Industrial Systems, School of Chemical Engineering and Analytical Science, The Mill, Sackville Street, The University of Manchester, Manchester M13 9PL, UK. E-mail: adisa.azapagic@manchester.ac.uk*
[b]*UK Centre for Carbon Dioxide Utilisation, Department of Chemical & Biological Engineering, Sir Robert Hadfield Building, The University of Sheffield, Sheffield, S1 3JD, UK*
[c]*Centre for Doctoral Training in Complex Particulate Products and Processes, School of Chemical & Process Engineering, University of Leeds, Leeds LS2 9JT, UK*
†Electronic supplementary information (ESI) available. See DOI: 10.1039/c9gc00732f

IL synthesis enable the design of task-specific ILs.[15] However, two key factors hinder their successful implementation for CO_2 capture at a commercial scale. Firstly, the high viscosity of ILs which are in the liquid state at room-temperatures (RTILs) results in extremely low CO_2 diffusion rates through the bulk liquid.[16] Even for low-viscosity RTILs, the diffusion rate is 19 orders of magnitude below that of MEA.[7] Secondly, the costs of RTILs remain high compared to other solvents. This is crucial since the low CO_2 diffusion rate means that very large quantities of ionic liquids are required in a capture plant, which in turn has negative implications for costs and the environmental footprint of the plant.

Organic salts with melting points significantly higher than room temperature have been proposed as an alternative to RTILs for applications such as CO_2 capture and energy storage.[17–21] These compounds have a somewhat contradictory name – 'solid ionic liquids' (SoILs) – as they are in the solid state at room temperature. In particular, methyltrioctyl ammonium acetate ($[N_{1888}][Ac]$), tetraethyl ammonium acetate ($[N_{4444}][Ac]$), tetra-octylammonium bromide ($[N_{8888}]Br$) and 1-butyl-4-methylimidazolium bromide ($[Bmim]Br$) have been investigated for CO_2 capture.[17] The rationale for the selection of these compounds relies on their high CO_2 uptake, ease of preparation and low cost of synthesis.[7] The aim of using such compounds is to alleviate the low CO_2 diffusion issues by the presence of large ionic surface areas. In contrast to the CO_2 capture methods of RTILs, SoILs are used in pressure swing adsorption (PSA) systems, which rely on a drop in pressure to release the more weakly-bound CO_2. PSA is an established process used in industry for gas or liquid separations.[22,23] Here, it is used to counteract the fact that, typically, crystalline and impermeable SoILs will not allow full gas–solid contact;[17] therefore, by applying a high pressure swing process, uptake capacities can be boosted by increasing gas–solid surface interactions.

Recently, cellulose has been suggested as a support for a range of SoILs. The motivation for this is the efficiency improvement through an increased ionic-surface area by cellulose coating, which in turn reduces the overall sorbent costs.[17] However, it is not clear if this also leads to a net CO_2 removal and an improved overall environmental performance of SoILs when taking into account the whole life cycle of the process. It is also unknown how they compare environmentally to RTILs and conventional CO_2 sorbents. Therefore, this paper evaluates the life cycle environmental sustainability of different SoILs, considering their production and use for CO_2 capture. A life cycle assessment (LCA) methodology has been used for these purposes, developed specifically to guide the sustainable development of novel ILs.[24] This is described in the next section, followed by the results in section 3 and the conclusions and recommendations for future work in section 4.

2 Methods

Life cycle data for ILs are scarce or non-existent owing to their limited use in industry or being available only at the laboratory
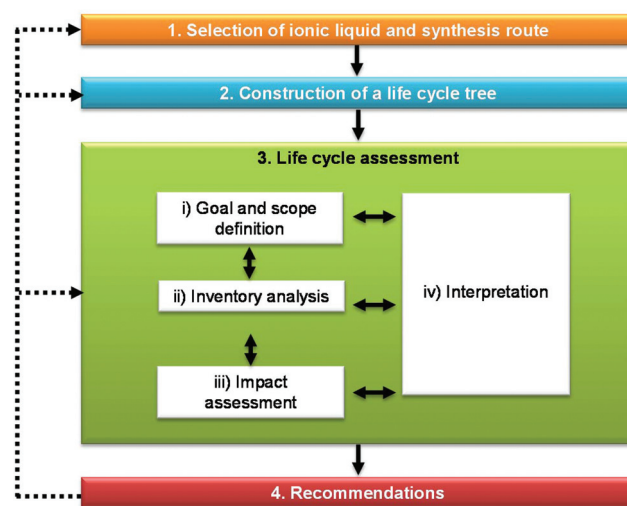

Fig. 1 Methodology for assessing the life cycle environmental sustainability of ionic liquids (adapted from Cuéllar-Franca *et al.*[24]).

scale. Furthermore, most ILs have complex chemical structures and numerous precursors are used in their production, for which environmental data are often lacking. To address this issue, a new LCA methodology was developed by Cuéllar-Franca *et al.*[24] which is applied in this study. This methodology helps to fill in data gaps and scale up laboratory data to industrial production, thus aiding the design of ILs under development and identification of more sustainable CO_2 sorbents.

As shown in Fig. 1, the methodology comprises four main steps which, when applied to SoILs, involve the following:

1. selection of SoILs and the synthesis route to be considered in the study;

2. construction of a life cycle tree showing the precursors used in the synthesis of the selected SoILs to enable the identification of data gaps and tracing back to the basic precursors for which life cycle data are available;

3. LCA of SoILs to estimate the environmental impacts of interest, identify hotspots and compare SoILs with other sorbents; and

4. recommendations for improvements, which can include a change of the synthesis route, substitution of raw materials, improvements in the energy and atom efficiency or selection of a different ionic liquid.

This process is iterative, with the recommendations fed back to the preceding steps, as needed. The following sections describe each of the above steps in more detail.

2.1 Selection of SoILs and synthesis route

The following four SoILs proposed previously for CO_2 capture[7,17] are assessed in this study with and without the cellulose support:

- methyltrioctyl ammonium acetate ($[N_{1888}][Ac]$);
- tetraethyl ammonium acetate ($[N_{4444}][Ac]$);
- tetra-octylammonium bromide ($[N_{8888}]Br$); and
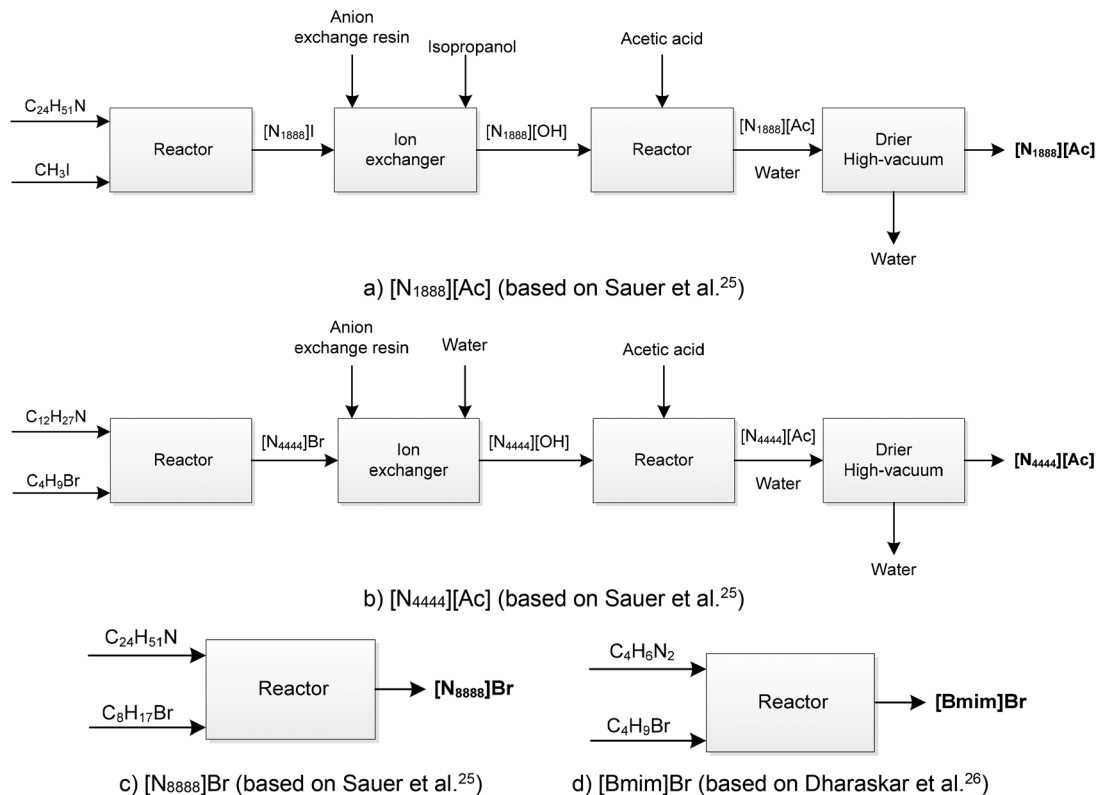- 1-butyl-4-methylimidazolium bromide ($[Bmim]Br$).

Fig. 2 Synthesis routes for the four SOILs considered in the study.

$[N_{1888}][Ac]$ is synthesised in three steps: production of quaternary tetraalkylammonium (amine quarterisation), anion exchange and reaction with acetic acid.[25] The synthesis process is depicted in Fig. 2a. In the first step, trioctylamine is mixed with methyl iodide in stoichiometric amounts at room temperature to yield methyltrioctylammonium iodide $[N_{1888}]I$.[25] The reaction is carried out using Schlenk-line techniques under an inert (N_2) atmosphere. Aluminium foil protection on the exterior of the reaction vessel and low lighting are used to prevent the decomposition of methyl iodine. In the second step, the anion exchange resin (Amberlite IRA resin) is regenerated with 1 M NaOH and rinsed with isopropanol. Then, $[N_{1888}]I$ prepared as in the previous step is dissolved in isopropanol and passed slowly through the resin, dropping directly into a flask. The product containing isopropanol and $[N_{1888}][OH]$ is passed through the column several times to exchange completely the iodide for the hydroxide anion.[25] Finally, $[N_{1888}][OH]$ is reacted with excess acetic acid and stirred for 16 hours at room temperature to yield $[N_{1888}][Ac]$, which is then dried in a rotary evaporator at 50 °C and under high vacuum (10 mbar) for 48 hours.

Similar to $[N_{1888}][Ac]$, $[N_{4444}][Ac]$ is also synthesised in three steps involving amine quarterisation, anion exchange and reaction with acetic acid[25] (Fig. 2b). In the first step, tributylamine is mixed stoichiometrically at room temperature with 1-bromobutane to yield tetrabutylammonium bromide, $[N_{4444}]Br$. The second and third steps are equivalent to the synthesis of $[N_{1888}][Ac]$, i.e. anion exchange followed by reaction with acetic

acid. The only difference between these two is that distilled water is used to dissolve $[N_{4444}]Br$ instead of isopropanol used for $[N_{1888}]I$.

$[N_{8888}]Br$ is synthesised by mixing trioctylamine with 1-bromooctane in the stoichiometric ratio at room temperature to obtain bromide salt[25] (Fig. 2c). Finally, [Bmim]Br is synthesised by mixing 1-methylimidazole with 1-bromobutane in stoichiometric amounts at 70 °C over 48 hours.[26] The synthesis process is shown in Fig. 2d.

The cellulose support for the ionic liquids is produced using wet coating techniques.[17] In this process, the ionic liquids are first dissolved in equal parts of methanol and isopropanol (5 litres of solvent per kg IL) before adding the required amount of cellulose. The alcohol solvents are removed by vacuum evaporation. Different cellulose loadings are considered, ranging from 70–80 wt% (i.e. 30% SoIL/70% cellulose to 20% SoIL/80% cellulose). This particular range of cellulose loadings has been chosen owing to the enhanced CO_2 adsorption capacity compared to lower or higher loadings.[17]

2.2 Life cycle tree of SoILs

Some of the compounds used in the synthesis of the SoILs considered in this study are not available in LCA databases. To overcome this issue, these compounds have been traced back to their main precursors through the construction of a life cycle tree for each SoIL, as shown in Fig. 3. As can be seen
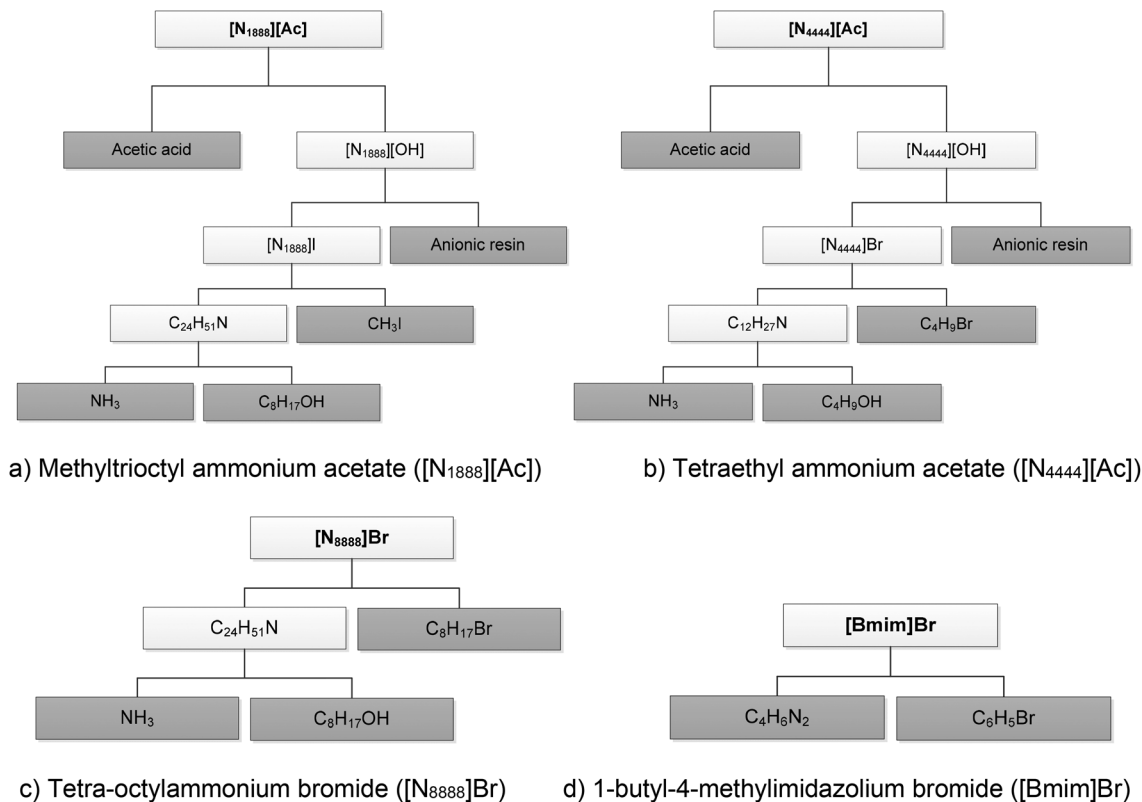
a) Methyltrioctyl ammonium acetate ([N$_{1888}$][Ac])

b) Tetraethyl ammonium acetate ([N$_{4444}$][Ac])

c) Tetra-octylammonium bromide ([N$_{8888}$]Br) d) 1-butyl-4-methylimidazolium bromide ([Bmim]Br)

Fig. 3 The life cycle tree for the production of SoILs considered in the study. (The dark-shaded boxes indicate the compounds for which data are available in LCA databases.)

from the figures, only the precursors for [Bmim]Br ($C_4H_6N_2$ and C_6H_5Br) are available in LCA databases (indicated as the dark-shaded boxes). For all others, there are significant data gaps, in most cases requiring tracing back to the basic precursors and their production processes. For example, the amines needed to synthesise both [N$_{1888}$]I (used as a precursor in N$_{1888}$[Ac]) and [N$_{4444}$]Br (a precursor for N$_{4444}$[Ac]) are traced back to ammonia and the alcohols used in their respective syntheses.[27,28]

2.3 Life cycle assessment of SoILs

The LCA has been carried out in accordance with the guidelines of the ISO 14040/14044 standards,[29,30] following the steps in Fig. 1. These are detailed in the next sections.

2.3.1 Goal and scope definition. The goals of the study are:

(i) to estimate the life cycle environmental impacts associated with the production of four selected SoILs, both with and without the cellulose support;

(ii) to identify environmental hotspots and opportunities for improvements and guide sustainable development of these sorbents at an early stage of development; and

(iii) to compare their impacts to other CO_2 sorbents and identify environmentally the most sustainable options; they are: a room-temperature ionic liquid trihexyl-tetradecylphosphonium 1,2,4-triazolide ([P$_{66614}$][124Triz]), monoethanolamine (MEA), zeolite powder and activated carbon.

For the first two goals, the system boundary is from "cradle to gate", which includes the extraction and manufacture of the raw materials used in the production of the precursors and SoILs, energy generation, transport and process waste management (Fig. 4). The unit of analysis (functional unit) is defined as the 'production of 1 kg of SoIL'.

For the third goal of the study, the use stage of the sorbents is also considered taking into account their adsorption capacities (Fig. 4). The functional unit in this case is 'adsorption of 1 kg of CO_2'. The impacts associated with the re-generation of the sorbents are excluded due to lack of specific data on PSA-SoIL systems. However, the effect of this assumption on the environmental impacts is assessed in the sensitivity analysis in section 3.2.2.4.

2.3.2 Inventory analysis. The primary data for the materials have been obtained from laboratory experiments.[17] These are detailed in Tables 2 and 3; for further details, see section S1 in the ESI.† The energy required for the production of SOILs has been estimated as detailed in section 2.3.2.2. The background life cycle inventory data for the materials and energy have been sourced from ecoinvent database v3.1.[31]

2.3.2.1 Materials. For some of the precursors, the life cycle inventory data were not available in the LCA databases; in such cases, data for alternative chemicals have been used as proxies. Specifically, data for methyl chloride have been used as a proxy for methyl iodide, 1-bromooctane and 1-bromobutane. This is a valid approximation since all these haloalkanes are syn-
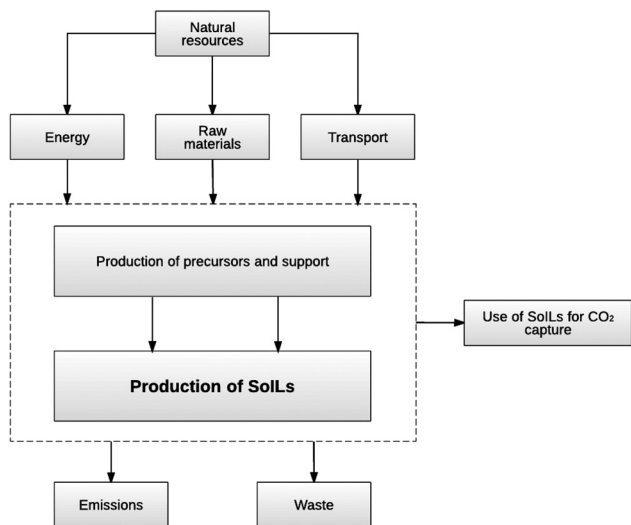
Fig. 4 System boundary for the production and use of SoILs. (All other sorbents considered in this study – zeolite, activated carbon, MEA and $[P_{66614}][124Triz]$ – have the same system boundary.)

thesised by thermal halogenation of the corresponding alkane by radical chain reaction at 300 °C.[32] In addition, fatty alcohols have been used instead of 1-octanol since the latter is a type of fatty alcohol. Finally, benzimidazole has been used for 1-methylimidazole since both are derived from imidazole. The

Table 1 CO_2 sorption capacities of SoILs and cellulose[17]

Sorbent	Capacity[a] (g CO_2 per kg sorbent)			
	$[N_{1888}][Ac]$	$[N_{4444}][Ac]$	$[N_{8888}]Br$	$[Bmim]Br$
Pure SoIL	28.6	14.9	1.7	12.3
70 wt% cellulose	16.7	21.2	19.8	16.1
75 wt% cellulose	30.0	31.6	19.2	28.8
80 wt% cellulose	14.9	25.7	15.8	24.9
Pure cellulose	4.8	4.8	4.8	4.8

[a] 298 K and 30 bar.

effect of these assumptions is tested through a sensitivity analysis in section 3.2.2.

The CO_2 adsorption capacities per unit mass of SoILs and pure cellulose are shown in Table 1.

In the absence of real operating data, it is assumed that the sorbent retains its adsorption capacity over 500 cycles, which is in line with a range of novel sorbents for CO_2 capture.[33,34] The effect of this assumption on the environmental impacts is also assessed in the sensitivity analysis in section 3.2.2.

All raw materials are assumed to be transported over a distance of 100 km to the corresponding production plant. The wastewater generated in the reaction between acetic acid and the quaternary ammonium hydroxide is assumed to be treated as industrial wastewater. The end-of-life disposal of SoILs is not considered due to lack of data. To gauge the effect of this assumption on the environmental impacts, end-of-life disposal is considered in the sensitivity analysis in section 3.2.2.5.

2.3.2.2   Energy. Given that the SoILs are still under development, data on energy consumption are not available and have been estimated as follows:

(i) the heat of formation of reactants and products has been used to estimate the theoretical energy requirements for the production of the SoILs and their precursors;

(ii) only the heat duty of the reactors (heating or cooling) has been considered. This means that the energy for separation, pumping and other operations is excluded from the calculations; the robustness of this assumption is tested in the sensitivity analysis in section 3.2.2; and

(iii) the theoretical duty of the reactors has been scaled up to an industrial scale using the empirical factors found in the literature[35] to account for energy efficiencies and losses; the theoretical duties have been multiplied by a factor of 4.2 in the case of exothermic reactions, assuming that natural gas is used as the source of heat, and multiplied by a factor of 3.2 in the case of endothermic reactions, assuming that electricity is used for cooling.[35]

Table 4 shows the estimated energy requirements by the reactors for the production of 1 kg of SoILs. Details on the cal-

Table 2 Chemical reactions involved in the synthesis of SoILs and their precursors

SoIL	Compound	Chemical reactions[a]	T (°C)	P (bar)
Methyltrioctyl ammonium acetate ($[N_{1888}][Ac]$)[b]	$[N_{1888}][Ac]$	$C_{25}H_{54}NOH + CH_3COOH \rightarrow \mathbf{C_{27}H_{57}NO_2} + H_2O$	25	1
	$[N_{1888}][OH]$	$C_{25}H_{54}IN + \bar{R}OH^- \rightarrow \mathbf{C_{25}H_{54}NOH} + \bar{R}I^-$	25	1
	$[N_{1888}]I$	$(C_8H_{17})_3N + CH_3I \rightarrow \mathbf{C_{25}H_{54}IN}$	75	1
	$(C_8H_{17})_3N$	$3C_8H_{17}OH + NH_3 \rightarrow \mathbf{(C_8H_{17})_3N} + 3H_2O$	230	100
Tetraethyl ammonium acetate ($[N4444][Ac]$)[b]	$[N_{4444}][Ac]$	$C_{16}H_{36}NOH + CH_3COOH \rightarrow \mathbf{C_{18}H_{39}NO_2} + H_2O$	25	1
	$[N_{4444}][OH]$	$C_{16}H_{36}BrN + \bar{R}OH^- \rightarrow \mathbf{C_{16}H_{36}NOH} + \bar{R}Br^-$	25	1
	$[N_{4444}]Br$	$(C_4H_9)_3N + C_4H_9Br \rightarrow \mathbf{C_{16}H_{36}BrN}$	75	1
	$(C_4H_9)_3N$	$3C_4H_9OH + NH_3 \rightarrow \mathbf{(C_4H_9)_3N} + 3H_2O$	230	100
Tetra-octylammonium bromide ($[N8888]Br$)[b]	$[N_{8888}][Br]$	$(C_8H_{17})_3N + C_8H_{17}Br \rightarrow \mathbf{C_{32}H_{68}BrN}$	75	1
1-Butyl-4-methylimidazolium bromide ($[Bmim]Br$)[c]	$[Bmim]Br$	$C_4H_6N_2 + C_4H_9Br \rightarrow \mathbf{C_8H_{15}BrN_2}$	70	1

[a] Bold font in the "Chemical reactions" column represents the chemical formula of the corresponding compound in the "Compound" column.
[b] Adapted from Sauer *et al.*[25] [c] Adapted from Dharaskar *et al.*[26]

Table 3 Materials used in the production of 1 kg of pure and cellulose-supported SoILs

		Amount (kg kg^{-1} SoIL)			
SoIL	Compound	Pure	70% cellulose	75% cellulose	80% cellulose
Methyltrioctyl ammonium acetate ([N$_{1888}$][Ac])	Acetic acid	0.146	0.044	0.037	0.029
	Methyl iodide[a]	0.333	0.100	0.083	0.067
	1-Octanol[b]	0.913	0.274	0.228	0.183
	Ammonia	0.040	0.012	0.010	0.008
	Anion exchange resin	0.034	0.010	0.009	0.007
	Isopropanol[c]	0.242	0.667	0.556	0.444
	Water[d]	0.197	0.059	0.049	0.039
	Cellulose	—	0.700	0.750	0.800
	Methanol[c]	—	0.594	0.495	0.396
Tetraethyl ammonium acetate ([N$_{4444}$][Ac])	Acetic acid	0.203	0.061	0.051	0.041
	1-Bromobutane[a]	0.455	0.137	0.114	0.091
	1-Butanol	0.738	0.221	0.184	0.147
	Ammonia	0.057	0.017	0.014	0.011
	Anion exchange resin	0.034	0.010	0.008	0.007
	Water[c]	0.242	0.073	0.061	0.049
	Water[d]	0.352	0.106	0.088	0.070
	Cellulose	—	0.700	0.750	0.800
	Methanol[c]	—	0.594	0.495	0.396
	Isopropanol[c]	—	0.594	0.495	0.396
Tetra-octylammonium bromide ([N$_{8888}$]Br)	1-Octanol[b]	0.714	0.214	0.178	0.143
	Ammonia	0.031	0.009	0.008	0.006
	1-Bromooctane[a]	0.354	0.106	0.088	0.071
	Cellulose	—	0.700	0.750	0.800
	Methanol[c]	—	0.594	0.495	0.396
	Isopropanol[c]	—	0.594	0.495	0.396
1-Butyl-4-methylimidazolium bromide ([Bmim]Br)	1-Methylimidazole[e]	0.375	0.113	0.094	0.075
	1-Bromobutane[a]	0.625	0.188	0.156	0.125
	Cellulose	—	0.700	0.750	0.800
	Methanol[c]	—	0.594	0.495	0.396
	Isopropanol[c]	—	0.594	0.495	0.396

[a] Methyl chloride used as a proxy. [b] Fatty alcohols used as a proxy. [c] Used as a solvent. [d] By-product. [e] Benzimidazole used as a proxy.

Table 4 Estimates of energy required by the reactors for the production of 1 kg of SoILs

SoIL	Compound	Theoretical energy consumption (MJ)	Scaled-up energy consumption (MJ)	Heating/cooling
Methyltrioctyl ammonium acetate ([N$_{1888}$][Ac])	[N$_{1888}$][Ac]	0.199	0.837	Heating
	[N$_{1888}$][OH]	N/A[a]	N/A[a]	N/A[a]
	[N$_{1888}$]I	0.203	0.851	Heating
	(C$_8$H$_{17}$)$_3$N	0.233	0.977	Heating
Tetraethyl ammonium acetate ([N4444][Ac])	[N$_{4444}$][Ac]	0.412	1.729	Heating
	[N$_{4444}$][OH]	N/A[a]	N/A[a]	N/A[a]
	[N$_{4444}$]Br	0.203	0.649	Cooling
	(C$_4$H$_9$)$_3$N	0.023	0.097	Heating
Tetra-octylammonium bromide ([N8888]Br)	[N$_{8888}$][Br]	0.532	2.232	Heating
1-Butyl-4 methylimidazolium bromide ([Bmim]Br)	[Bmim]Br	0.388	1.240	Cooling

[a] N/A: not applicable as the anion exchange reaction does not involve heating or cooling.

culation of the heat duty of the reactors can be found in section S2 in the ESI.† In all estimates, electricity is assumed to be supplied from the UK grid at medium voltage while heat is assumed to be supplied by steam generated from natural gas.

The energy consumption of PSA systems for CO$_2$ capture has been reported in the range of 331–724 kJ kg^{-1} CO$_2$,[23]

depending on the process configuration, gas composition, operating conditions and the type of adsorbent. However, the PSA system is not considered in the study as the energy consumption would be nearly identical across the sorbents. Nevertheless, a sensitivity analysis is included in section 3.2.2.4 to assess the effect of this assumption on the environmental impacts.

3 Results and discussion

3.1 Impact assessment

The LCA software Gabi v6.4 [36] has been used to model the systems and estimate the environmental impacts, following the CML 2001 impact assessment methodology (April 2015 update).[37] The CML methodology has been selected to allow comparison with the room-temperature IL $[P_{66614}][124Triz]$ for which LCA data were published previously.[24] The following 11 impacts included in the CML method are considered: global warming potential (GWP), abiotic depletion potential for elements (ADP elements), abiotic depletion potential for fossil resources (ADP fossil), acidification potential (AP), eutrophication potential (EP), human toxicity potential (HTP), ozone layer depletion potential (ODP), photochemical oxidants creation potential (POCP), fresh water and marine aquatic eco-toxicity potential (FAETP and MAETP) and terrestrial eco-toxicity potential (TETP).

The results are first discussed for the functional unit related to the production of 1 kg of SoILs, followed by the impacts per 1 kg of CO_2 captured.

3.1.1 Functional unit: 1 kg of SoIL.
The results for the cellulose-supported SoILs are shown in Fig. 5 in comparison with pure SoILs. For reference, the impacts of pure cellulose are also given, showing that they have significantly lower impacts than the pure and supported SoILs. For this reason, the supported SoILs have in general lower impacts per kg of adsorbent than the pure SoILs. For instance, the GWP of the supported SoILs is estimated in the range of 1.9–2.4 kg CO_2-eq. and for the pure sorbents at 2.4–4.9 kg CO_2-eq. The impacts decrease linearly as the cellulose loading increases. This linear relationship can be explained by the fact that pure cellulose has significantly lower impacts than pure SoILs and, consequently, the addition of cellulose will generally result in a reduction of the impacts of the sorbent in direct proportion to the amount of cellulose added, displacing the equivalent amount of SoIL. However, some impacts are higher for the supported adsorbents. For instance, supported $[N_{1888}][Ac]$ and $[N_{8888}][Br]$ have higher ADP fossil and EP than their unsupported equivalents. This is due to the positive effect of the cellulose being outweighed by the use of methanol and isopropanol needed to dissolve the SoIL during the cellulose-coating process. As the cellulose loading increases, the amount of methanol/isopropanol required decreases since this is proportional to the amount of SoIL to be dissolved; therefore, the effect of solvents on the impact is smaller and the impacts are lower.

Comparing the four supported types of SoILs, it can be seen in Fig. 6a that [Bmim]Br has the highest and $[N_{8888}]$Br the lowest impacts for the vast majority of the categories considered. The difference in impacts between them ranges from 22% for GWP to 86% for HTP in favour of $[N_{8888}]$Br. The main reason for the poor environmental performance of [Bmim]Br is the use of 1-methylimidazole, which has higher impacts than any other precursor used for any of the other SoILs assessed. The only exceptions to the trends regarding [Bmim]Br are ADP fossil and ODP, which are the highest for

$[N_{4444}][Ac]$. For $[N_{8888}]$Br, the exceptions are HTP and TETP which are slightly lower for $[N_{4444}][Ac]$. A similar trend is also found for the pure SoILs (see Fig. S1 in section S3 in the ESI†).

3.1.2 Functional unit: 1 kg of CO_2 adsorbed.
When the adsorption capacities of the SoILs are taken into account, the supported SoILs also have lower impacts than their pure counterparts in all the impact categories (Fig. 5). The only exception to this is $[N_{1888}][Ac]$ with 80% cellulose ($[N_{1888}][Ac]$-80%) which has higher impacts than the pure sorbent across the categories, except for ADP elements, ODP and TETP.

The impacts per kg CO_2 adsorbed decrease as the cellulose loading increases for $[N_{4444}][Ac]$ and [Bmim]Br. This is due to the lower impacts of producing the cellulose and also the higher adsorption capacity of the supported SoILs compared to the pure sorbents. As opposed to the impacts per kg of SoIL discussed in section 3.1.1, the relationship between the cellulose loading and a decrease in the impacts is no longer linear. This is due to the competitive effects of the lower impacts of producing the cellulose versus a lower adsorption capacity of the supported SoILs at 80% loading compared to 75%. For $[N_{1888}][Ac]$, the impacts increase at a cellulose loading of 70% due to a decrease in the adsorption capacity at this level of loading. The impacts then decrease when the loading increases to 75% to increase once again for 80% loading. This is the result of the adsorption capacity showing a maximum at 75% cellulose loading, which can be explained by a smoother coating of the IL on the fibrous cellulose particle at this loading level.[17] The impacts of $[N_{8888}]$Br are at a minimum at 75% cellulose loading, even though the highest adsorption capacity is at 70% cellulose loading. This is due to a greater effect of the lower impacts of producing the cellulose versus the slightly lower adsorption capacity at 75% loading.

All the supported sorbents have a net GWP below 1 kg CO_2 eq. kg^{-1} CO_2 adsorbed, ranging from 0.167 kg CO_2 eq. for $[N_{1888}][Ac]$ to 0.233 kg for $[N_{8888}]$Br at 75% loading (Fig. 6b). This means that they remove more CO_2 eq. than they generate; however, their net carbon removal efficiency is 77%–83%. A similar trend is found for the pure SoILs, but with a lower removal efficiency (20%–76%). The only exception is pure $[N_{8888}]$Br which generates almost three times more CO_2 eq. (2.8 kg) for each kg it removes (Fig. 5).

With respect to the other impacts, $[N_{4444}][Ac]$-80% is the best option for eight out of 11 categories (Fig. 6b). This is due to its higher adsorption capacity compared to the other SoILs (Table 1). For the remaining three impacts, $[N_{1888}][Ac]$-75% is the best sorbent for GWP and ADP fossil, while $[N_{8888}]$Br-75% outperforms the others for ODP.

3.2 Interpretation of results

3.2.1 Environmental hotspots and improvement opportunities.
Raw materials are responsible for over 90% of the total impact across the categories. In the case of $[N_{1888}][Ac]$, the isopropanol and methanol used to dissolve the cellulose contribute over 52%–55% of the total GWP depending on the cellulose loading, while the cellulose

Fig. 5 Environmental impacts of pure and cellulose-supported SoILs as a function of cellulose loading: per kg of adsorbent (left) and per kg CO_2 adsorbed (right). (For impacts nomenclature, see section 3.1. The error bars represent the 70% (upper limit) and 80% cellulose loading (lower limit), except for [N$_{1888}$][Ac] and [N$_{8888}$][Ac], for which the error bars represent 70% (upper limit) and 75% cellulose loading (lower limit). Some impacts have been scaled to fit − to obtain the original values, multiply by the factor shown on the x-axis.)

itself contributes around 10% of the total GWP. Isopropanol is also the main hotspot for all other environmental categories but ODP. The latter is due to the anion resin used in the production of [N$_{1888}$][Ac] from [N$_{1888}$]I, contributing 55% of the total ODP. This is despite the small amount of the resin (34.5 g kg^{-1} [N$_{1888}$][Ac]). The reason for this particularly high contribution to ODP is the

trichloromethane used in the manufacturing of the resin. A further significant contributor to the ODP is methyl iodide, causing 37% of the total ODP. Owing to the nature of the synthesis routes, similar trends to those of [N$_{1888}$][Ac] are observed for the environmental hotspots of [N$_{4444}$][Ac], with the only difference being the use of 1-butanol instead of 1-octanol.
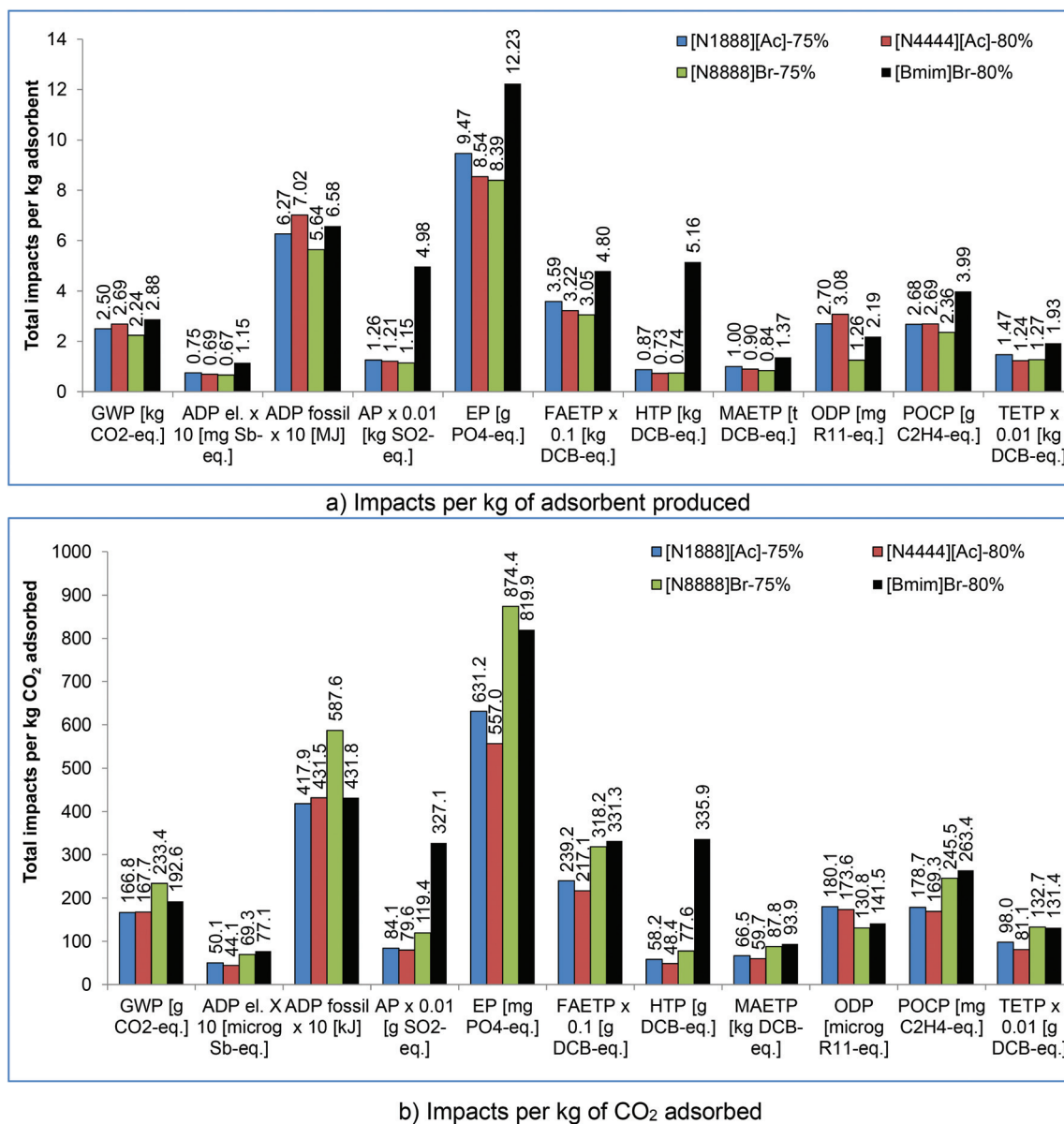
Fig. 6 Comparison of the best-performing SoILs for different functional units. (For impacts nomenclature, see section 3.1. Some impacts have been scaled to fit − to obtain the original values, multiply by the factor shown on the x-axis.)

Isopropanol and methanol for cellulose dissolution are also the main contributors to all the impacts related to [N$_{8888}$]Br, except for ODP. For instance, they contribute 56%–59% of the total GWP, while cellulose contributes 15% of the impact. 1-Methylbromide is the main hotspot for ODP with a contribution of 84% of the total ODP. For [Bmim]Br, the main contributors are again isopropanol and methanol for cellulose dissolution. For instance, they contribute 42%–44% of the GWP and over 60% of the toxicity-related impacts. 1-Methylimidazole is also an important hotspot since it causes 25% of the GWP and over 30% of all other impacts but ADP fossil and ODP.

Although energy required for heating/cooling of the reactors is the second largest contributor to the impacts from the SoILs, its share is significantly smaller than that of the raw materials. As an example, energy contributes 4%–6% of the GWP across the SoIL types. The contribution of transport and wastewater treatment is negligible, with the shares of <1% and 0.01%, respectively.

Therefore, the hotspot analysis suggests that the main opportunities for improvements are related to reducing the impacts associated with the SoIL precursors. This can be achieved by replacing them with other precursors with lower environmental impacts or developing alternative synthesis routes. Fatty alcohols, such as 1-octanol used in the synthesis of trioctylamine (a precursor to [N$_{1888}$][Ac] and [N$_{8888}$]Br), are significant contributors to most environmental impacts. Therefore, they should be replaced by alcohols from bio-

sources, such as coconut oil. For example, the latter has the GWP of 1.41 kg CO_2 eq. kg^{-1} compared to 2.56 kg CO_2 eq. kg^{-1} of alcohol from petrochemical origin.[31] Furthermore, the use of SoILs that involve imidazole-derived precursors, as in the case of [Bmim]Br, should be avoided because of their high environmental impacts, including GWP (7.52 kg CO_2 eq. kg^{-1} (ref. 31)). Furthermore, using anion resins that do not rely on trichloromethane could reduce the ODP.

3.2.2 Sensitivity analysis. To examine the effect on the impacts of some of the assumptions, the following is considered in the sensitivity analysis:

(i) use of proxy data for some raw materials (Table 3);

(ii) estimates of energy consumption for SoIL synthesis (Table 4);

(iii) the number of adsorption/desorption cycles;

(iv) electricity consumption by the PSA unit; and

(v) the end-of-life disposal of the spent SoILs.

3.2.2.1 The effect of proxy data for raw materials. As discussed in section 2.3.2.1, alternative chemicals have been used as proxies for those compounds for which life cycle inventory data are not available. The effect of this assumption is tested by varying the impacts of these materials (arbitrarily) by ±50%. As the raw materials are relevant to the production rather than the use of the sorbents, the analysis is carried out for the functional unit related to the production of 1 kg of the SoILs. The results for 75% cellulose loading are given in Fig. 7 and for the other two loadings in Fig. S2 and S3 in the ESI.† For instance,

a 50% increase in the impacts of the proxy raw materials assumed to be used in the production of SoILs with 75% cellulose results in an average increase in the GWP of 13%. Similar trends are found for the other impacts across the SoIL types, except for [Bmim]Br which shows a greater sensitivity to the assumptions for the raw materials (Fig. 7). For example, a 50% higher GWP of the proxy raw materials leads to a 20% increase in the overall GWP of [Bmim]Br, whereas for the other three SoILs the increase ranges from 6% to 12%. This is due to the higher environmental impacts of benzimidazole, which is used as a proxy for 1-methylimidazole (Table 3). Similar trends are observed for 70% and 80% cellulose loadings (Fig. S2 and S3†).

3.2.2.2 The effect of energy consumption for SoIL synthesis. As discussed in section 2.3.2.2, energy consumption by the reactor to produce the SoILs had to be estimated due to lack of data. Here, these estimates are varied by ±50% to gauge the effect on the overall impacts per kg of sorbent produced. As can be seen in Fig. S4 in the ESI† for the SoILs with 75% cellulose loading, the impacts are not sensitive to these changes. For example, a 50% increase in the energy consumption results in an average increase of 0.8% of the GWP across the SoILs. A similar trend applies for the other impacts.

3.2.2.3 The effect of adsorption/desorption cycles. The number of adsorption/desorption cycles is varied from 100–1000 in the sensitivity analysis, from 500 considered in the base case. It is assumed that the adsorption capacity of the
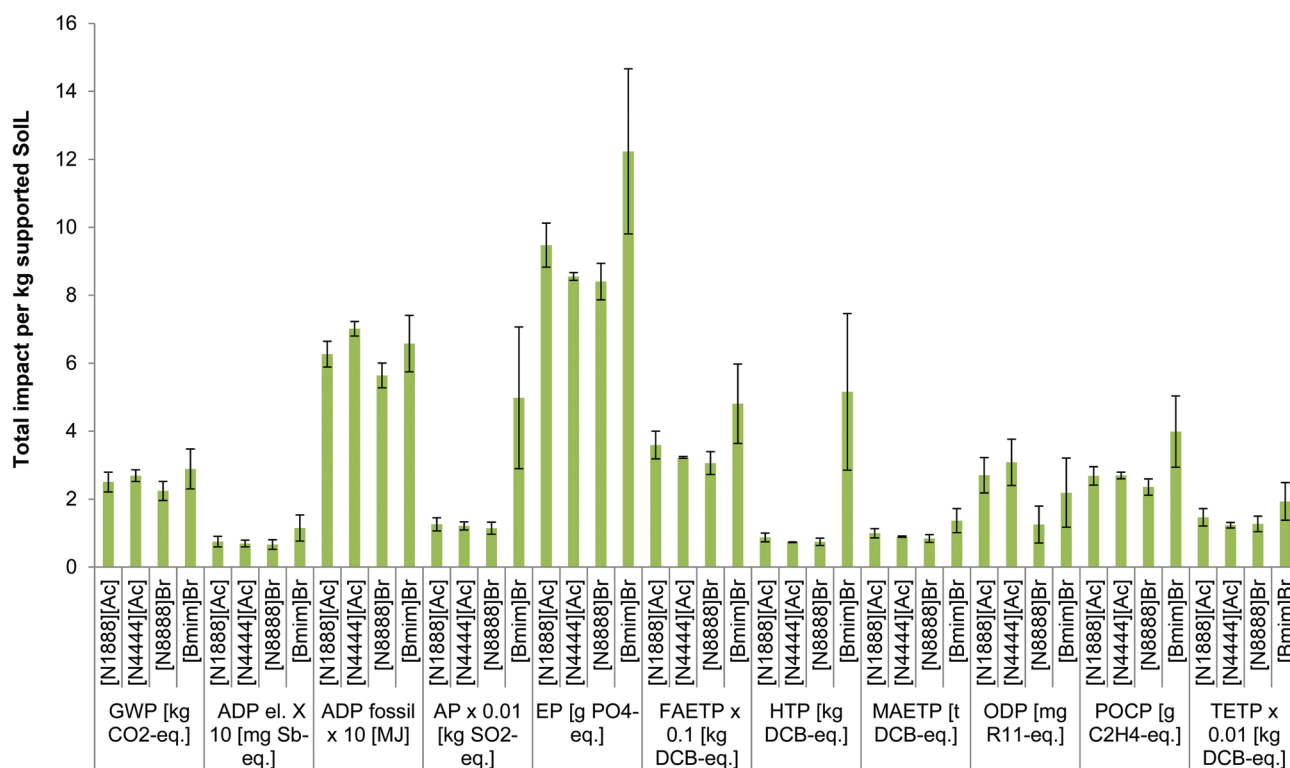

Fig. 7 Sensitivity analysis for the assumptions on the raw materials used in the production of the SoILs with 75% cellulose loading. (The graph bars represent the impacts in the base case and the error bars the impacts for the ± variation in impacts of the proxy raw materials. For impacts nomenclature, see section 3.1. Some impacts have been scaled to fit – to obtain the original values, multiply by the factor shown on the x-axis.)
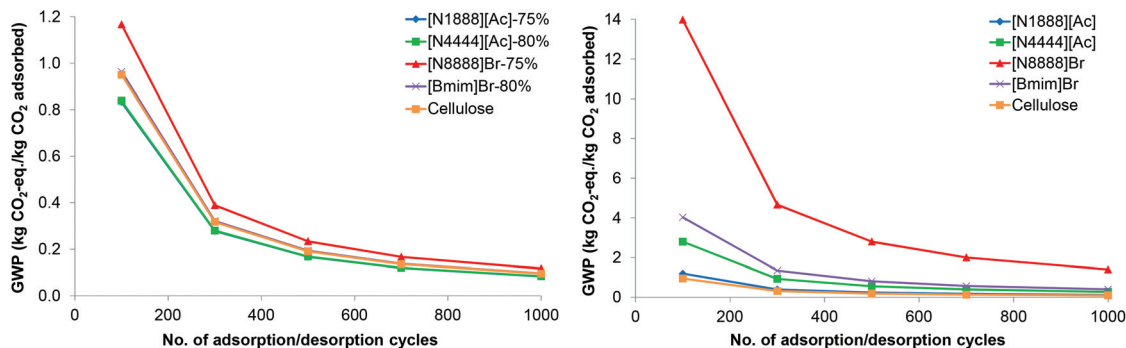
Fig. 8 Effect of the adsorption/desorption cycles on global warming potential (GWP) of the best-performing SoILs with cellulose (left) and pure SoILs (right). (75% and 80% in the legend denote the level of cellulose loading. Pure cellulose is also shown on both graphs for context.)

sorbents remains constant in all cycles. Given that this analysis is related to the use of the sorbents, the functional unit is related to 1 kg of adsorbed CO_2. An example effect on the impacts is shown in Fig. 8 for GWP for the best-performing SoILs and for pure sorbents. Note that the values for GWP of the supported $[N_{4444}][Ac]$ and $[N_{1888}][Ac]$ are the same and cannot be differentiated as shown in Fig. 8 (left); the same applies to the supported $[Bmim]Br$ and pure cellulose. As can be seen, the GWP decreases exponentially as the number of cycles increases for both supported and unsupported SoILs. This is due to a longer lifespan of the sorbents and the higher overall amount of CO_2 captured during their lifetime. For these optimal levels of cellulose loading, pure SoILs have higher GWP than the supported SoILs across the range of cycles.

These results can also be used to determine the number of cycles over which a SoIL will need to retain its adsorption capacity to outperform other sorbents, including the cellulose. For instance, $[N_{8888}]Br$-75% will outperform pure cellulose if it can be used in more than 200 cycles if cellulose lasts for only 100 cycles. For the same number of cycles, $[N_{1888}][Ac]$-75% outperforms the rest of the supported sorbents and the cellulose. Nevertheless, its GWP remains net positive across the adsorption cycles, but it halves from 0.167 to 0.083 kg CO_2 eq. kg^{-1} CO_2 adsorbed as the number of cycles doubles from 500 to 1000. The other impacts are also similarly sensitive to the number of adsorption/desorption cycles.

3.2.2.4   The effect of electricity consumption by the PSA unit. Electricity consumption by the PSA unit has not been considered in the base case due to lack of data. The effect of this assumption is tested here by comparing the impacts in the base case with a low and high PSA energy consumption (331 and 724 kJ kg^{-1} CO_2 adsorbed, respectively) reported in the literature.[23] It can be seen in Fig. 9 that most impacts are unaffected or increase only slightly when the PSA electricity is considered. The exception to this is GWP, which is 20%–66% higher across the SoILs. ADP fossil and AP also increase, by 11%–33% and 7%–49%, respectively. However, the environmental ranking of the SoILs remains the same as in the base case.

3.2.2.5   The effect of end-of-life disposal of the spent SoILs. End-of-life disposal of the SoILs has not been considered in

the base case due to lack of data. To find out if this exclusion would affect the overall impacts, it is assumed in the sensitivity analysis that the SoILs are landfilled as hazardous materials. The results in Fig. 10 suggest that in that case the effect on most impacts is negligible, except for FAETP and MAETP which increase respectively by 17%–25% and 14%–22% across the SoILs. HTP also increases by 10%–15% with the exception of $[Bmim]Br$-80%, where it increases only by 2%. Given a similar effect on the impacts of the SoILs' end-of-life, their ranking in terms of the environmental performance remains the same as in the base case.

3.2.3   Comparison with other sorbents. The environmental impacts of SoILs are compared to the room-temperature IL $[P_{66614}][124Triz]$, MEA, zeolite powder and activated carbon. $[P_{66614}][124Triz]$ has been selected here as one of the promising ILs for CO_2 capture[38] and the MEA since this is the most prevalent sorbent used in commercial CO_2 capture. Zeolite powder and activated carbon are considered because they have been widely reported as suitable, commercially available adsorbents for CO_2 capture in PSA systems.[39–41] The terms "zeolites" and "activated carbon" are generic names used to designate families of materials that have similar composition but different internal structures, pore sizes and surface areas; therefore, average values of the adsorption capacity of different zeolites and activated carbons have been calculated using the adsorption capacities shown in Table 5.

The LCA impacts of both MEA and $[P_{66614}][124Triz]$ per kg of CO_2 captured have been sourced from Cuéllar-Franca *et al.*[24] The environmental impacts of the zeolite powder are from the ecoinvent database and the data for the activated carbon are from Bayer *et al.*[42] The activated carbon is assumed to be produced from coal, which is the most prevalent feedstock for activated carbon in industry.[43] It is assumed that 99.997% of MEA and $[P_{66614}][124Triz]$ is recycled in the process after regeneration.[24] The SoILs, zeolite and activated carbon are assumed to undergo 500 adsorption/desorption cycles with their respective adsorption capacities remaining constant over their lifetime. The effect of the number of adsorption cycles on the impacts is explored further below.

The environmental impacts of these four sorbents are compared in Fig. 11 with $[N_{4444}][Ac]$-80% per kg of CO_2 adsorbed.
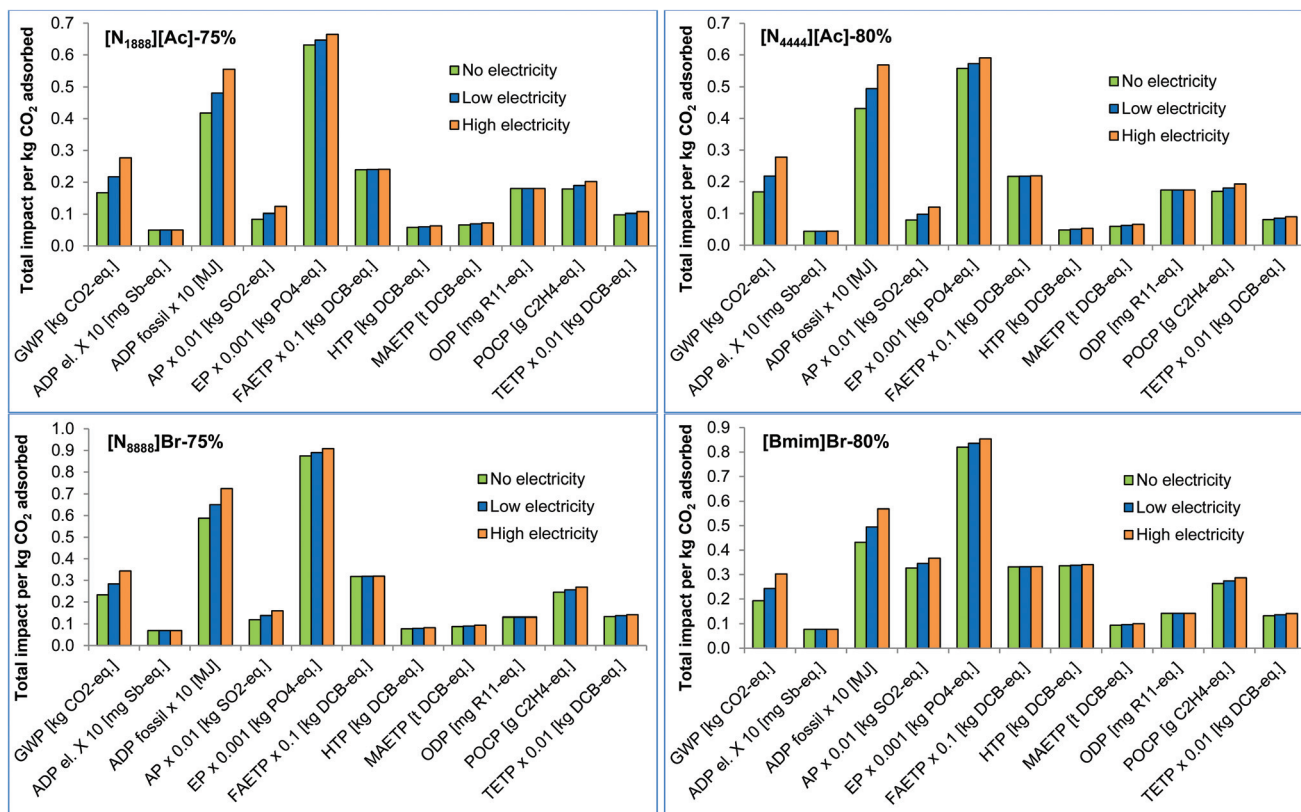
Fig. 9 Effect of energy consumption by the PSA unit on the impacts of SoILs. (The low and high electricity consumption correspond to 331 and 724 kJ kg^{-1} CO_2 adsorbed, respectively. For impacts nomenclature, see section 3.1.)
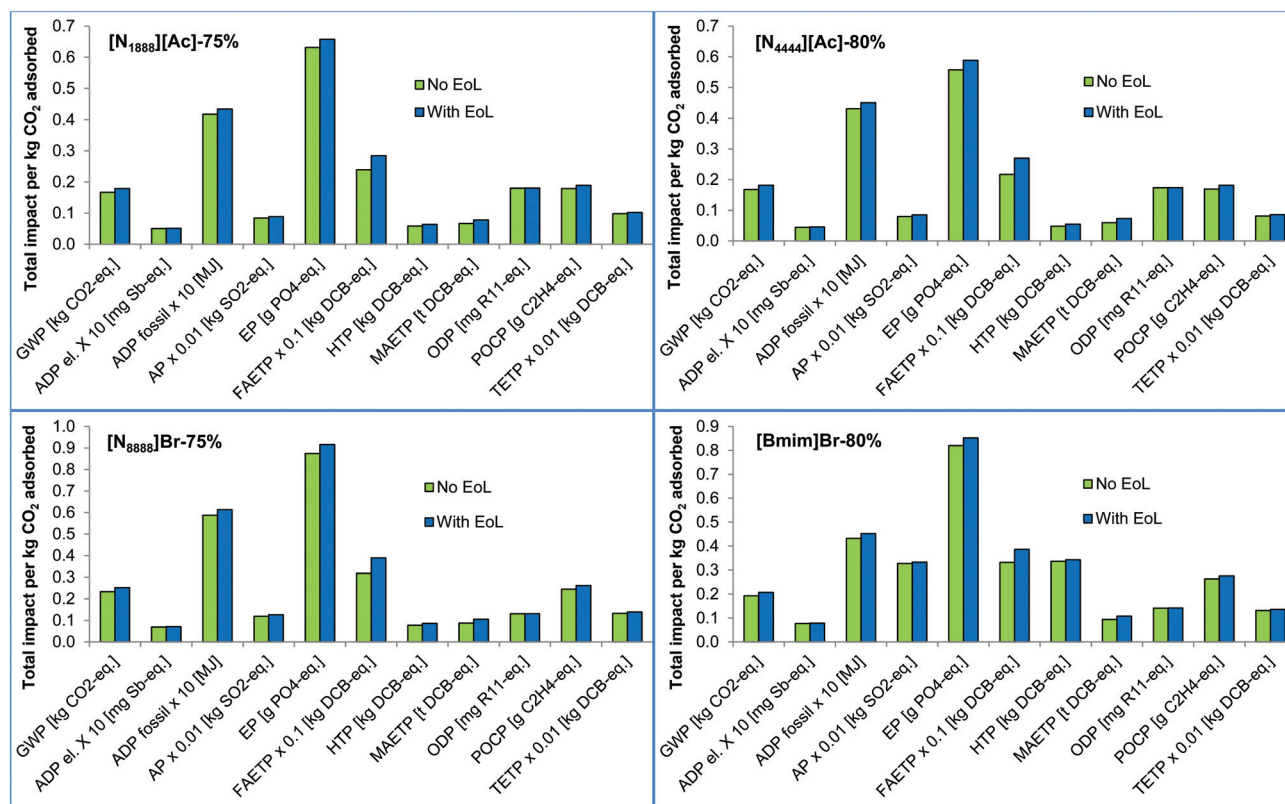

Fig. 10 Effect of end-of-life disposal on the impacts of SoILs. (For impacts nomenclature, see section 3.1. EoL: end of life.)

Table 5 CO_2 adsorption capacities of different activated carbons, zeolites, MEA, $[P_{66614}][124Triz]$ and $[N_{4444}][Ac]$

Adsorbent type	Adsorbent name	Adsorption capacity (kg CO_2 kg^{-1} adsorbent)	Source
Activated carbon	Norit R1	0.440	Himeno et al.[44]
	BPL	0.334	~II~
	A10	0.378	~II~
	AC A	0.334	~II~
Zeolite	Zeolite 13X	0.220	Zhang et al.[45]
	Zeolite 13X	0.308	Cavenati et al.[46]
Amine	MEA	0.295	Sønderby et al.[47]
Room-temp. IL	$[P_{66614}][124Triz]$	0.081^a	Taylor et al.[38]
SoIL	$[N_{4444}][Ac]$-80% cellulose	0.026^b	Reed et al.[17]

^{a} 298 K and 1 bar. ^{b} 298 K and 30 bar.

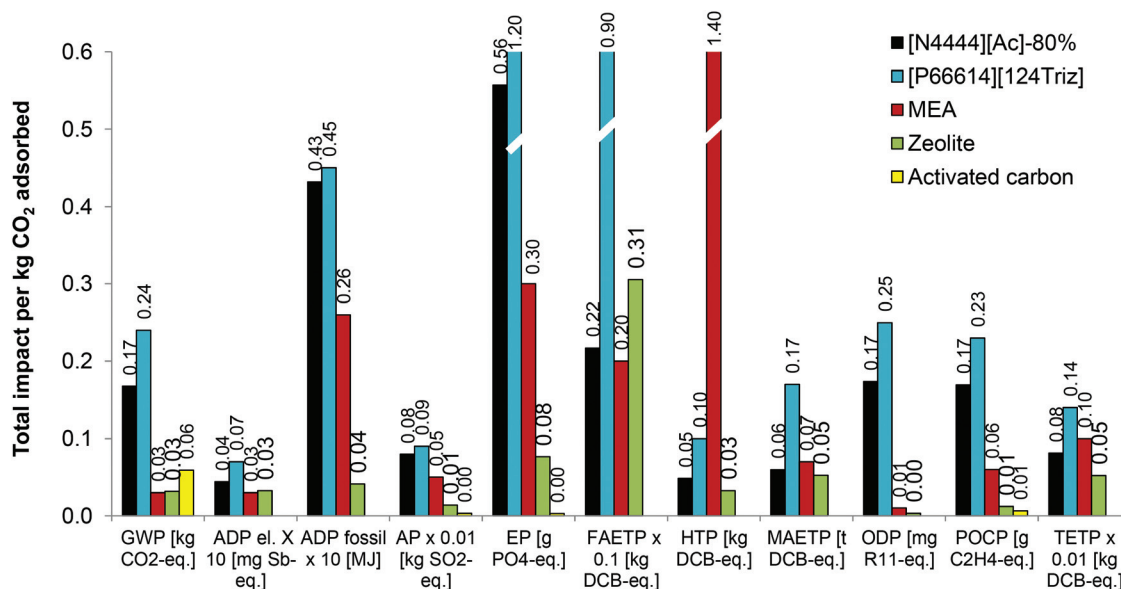**Fig. 11** Comparison of environmental impacts of different sorbents. (Assumptions: 99.997% regeneration of MEA and $[P_{66614}][124Triz]$ and 500 adsorption/desorption cycles for $[N_{4444}][Ac]$-80%, zeolite and activated carbon. For impacts nomenclature, see section 3.1.)

This SoIL is considered for comparison because it has the lowest impacts of all the SoILs considered in eight out of 11 categories.

The results suggest that, compared to $[P_{66614}][124Triz]$, $[N_{4444}][Ac]$-80% has lower impacts for all the categories, ranging from 4% lower ADP fossil to 76% lower FAETP. In comparison with MEA, $[N_{4444}][Ac]$-80% has higher impacts, except for HTP, MAETP and TETP, which are 97%, 15% and 19% lower than for MEA, respectively. The rest of its impacts are between 9% (FAETP) and 17 times higher (ODP) than for MEA.

Compared with zeolite powder, $[N_{4444}][Ac]$-80% is a worse option for 10 out of 11 impacts, ranging from 14% higher MAETP to 55 times greater ODP. The latter is particularly high for $[N_{4444}][Ac]$-80% owing to the trichloromethane used in the preparation of the anionic resin as well as the methyl iodide used as a precursor in the synthesis of $[N_{4444}][Ac]$. On the other hand, $[N_{4444}][Ac]$-80% has lower FAETP than zeolite.

$[N_{4444}][Ac]$-80% is also less environmentally sustainable than activated carbon for all four impacts available for the latter: it has three times higher GWP, 25 times greater AP, 26 times higher POCP and 199 times greater EP (Fig. 11). The reason for a particularly high EP is the phosphoric acid diatomite used as a catalyst in the production of isopropanol via the direct hydration of propene. Since large amounts of isopropanol are needed to dissolve the cellulose, its effect on EP is exacerbated.

The effect of the number of adsorption/desorption cycles on the impacts is shown in Fig. 12 through the example of GWP. As can be seen, $[N_{4444}][Ac]$-80% has a higher GWP than activated carbon and zeolite powder for the same number of cycles. However, it has a lower GWP than activated carbon as long as it retains its adsorption capacity for at least 300 cycles and the activated carbon for 100 cycles. Alternatively, the SoIL would have to retain its adsorption capacity for at least 500 cycles in order to outperform zeolite powder if the latter only
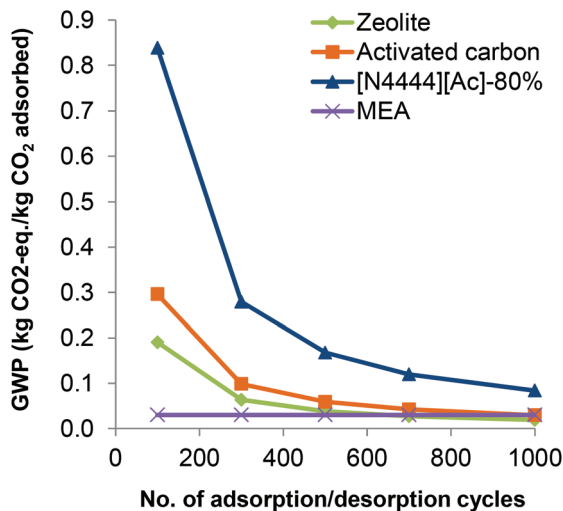
Fig. 12 Effect of adsorption/desorption cycles on the global warming potential (GWP) of $[N_{4444}][Ac]$-80%, activated carbon and zeolite powder.

lasts for 100 cycles. Fig. 12 also shows that $[N_{4444}][Ac]$-80% has higher GWP than MEA across the number of cycles considered.

4 Conclusions

This work has estimated for the first time the life cycle environmental impacts of four novel cellulose-supported SoILs in comparison with their pure counterparts and some conventional CO_2 sorbents, such as MEA, zeolite and activated carbon. The results indicate that the supported SoILs have lower impacts per kg CO_2 adsorbed than pure SoILs in all the impact categories. The only exception is $[N_{1888}][Ac]$-80% which has higher impacts than the pure sorbent across the categories, except for ADP elements, ODP and TETP. For all four SoILs, raw materials are the main contributors to environmental impacts.

All the supported SoILs have a net GWP below 1 kg CO_2 eq. kg^{-1} CO_2 captured, meaning that they remove more CO_2 eq. than they generate. However, their net carbon removal efficiency is 77%–83%. A similar trend is found for the pure SoILs, but with a lower removal efficiency of 20%–76%. The only exception is pure $[N_{8888}]Br$ which generates almost three times more CO_2 eq. for each kg it removes.

$[N_{4444}][Ac]$-80% is the best SoIL for eight out of 11 impact categories. For the remaining three impacts, $[N_{1888}][Ac]$-75% is the best sorbent for GWP and ADP fossil, while $[N_{8888}]Br$-75% outperforms the others for ODP.

In comparison to other CO_2 sorbents, the best supported SoIL – $[N_{4444}][Ac]$-80% – is environmentally more sustainable than $[P_{66614}][124Triz]$ but it has significantly higher impacts than MEA, zeolite and activated carbon.

The results presented in this work can guide the further development of environmentally more sustainable solid ionic liquids for CO_2 capture. However, real data on the adsorbent recyclability, operating conditions and unit operations involved in the CO_2 capture by SoILs will be required to determine whether such processes can be environmentally more sustainable than those using conventional sorbents, such as activated carbon, zeolites or MEA. Furthermore, as SoILs have a low CO_2 adsorption capacity, future studies should also evaluate the economic sustainability of their potential commercial application.

Conflicts of interest

There are no conflicts of interest to declare.

Acknowledgements

References

1 European Academies Science Advisory Council, *Carbon capture and storage in Europe*, German National Academy of Sciences Leopoldina, Halle (Saale), Germany, 2013.

2 J. D. Figueroa, T. Fout, S. Plasynski, H. McIlvried and R. D. Srivastava, *Int. J. Greenhouse Gas Control*, 2008, **2**, 9–20.

3 P. Styring, D. Jansen, H. de Coninck, H. Reith and K. Amstrong, *Carbon Capture and Utilisation in the Green Economy*, The Centre for Low Carbon Futures, Yotk, 2011.

4 R. J. Notz, I. Tönnies, N. McCann, G. Scheffknecht and H. Hasse, *Chem. Eng. Technol.*, 2011, **34**, 163–172.

5 E. S. Rubin, H. Mantripragada, A. Marks, P. Versteeg and J. Kitchin, *Prog. Energy Combust. Sci.*, 2012, **38**, 630–671.

6 L. Zhu, G. W. Schade and C. J. Nielsen, *Environ. Sci. Technol.*, 2013, **47**, 14306–14314.

7 G. R. M. Dowson, D. G. Reed, J.-M. Bellas, C. Charalambous and P. Styring, *Faraday Discuss.*, 2016, **192**, 511–527.

8 M. R. M. Abu-zahra, P. H. M. Feron and G. F. Versteeg, *Int. J. Greenhouse Gas Control*, 2007, **1**, 37–46.

9 J. Kittel, R. Idem, D. Gelowitz, P. Tontiwachwuthikul, G. Parrain and A. Bonneau, *Energy Procedia*, 2009, **1**, 791–797.

10 X. Zhang, X. Zhang, H. Dong, Z. Zhao, S. Zhang and Y. Huang, *Energy Environ. Sci.*, 2012, **5**, 6668.

11 J. S. Wilkes, P. Wasserscheid and T. Welton, in *Ionic Liquids in Synthesis*, Wiley-VCH Verlag GmbH & Co. KGaA, Weinheim, Germany, 2007, pp. 1–6.

12 J. F. Brennecke and B. E. Gurkan, *J. Phys. Chem. Lett.*, 2010, **1**, 3459–3464.

13 R. G. Reddy, *J. Phys.: Conf. Ser.*, 2009, **165**, 012076.

14 C. Maton, N. De Vos and C. V. Stevens, *Chem. Soc. Rev.*, 2013, **42**, 5963.

15 B. Lee and S. Lin, *Chem. Eng. Sci.*, 2015, **121**, 157–168.

16 C. Moya, J. Palomar, M. Gonzalez-Miquel, J. Bedia and F. Rodriguez, *Ind. Eng. Chem. Res.*, 2014, **53**, 13782–13789.

17 D. G. Reed, G. R. M. Dowson and P. Styring, *Front. Energy Res.*, 2017, **5**, 13.

18 D. R. MacFarlane, M. Forsyth, P. C. Howlett, M. Kar, S. Passerini, J. M. Pringle, H. Ohno, M. Watanabe, F. Yan, W. Zheng, S. Zhang and J. Zhang, *Nat. Rev. Mater.*, 2016, **1**, 15005.

19 J. Wang, L. Huang, R. Yang, Z. Zhang, J. Wu, Y. Gao, Q. Wang, D. O'Hare and Z. Zhong, *Energy Environ. Sci.*, 2014, **7**, 3478–3518.

20 S. Zeng, X. Zhang, L. Bai, X. Zhang, H. Wang, J. Wang, D. Bao, M. Li, X. Liu and S. Zhang, *Chem. Rev.*, 2017, **117**, 9625–9673.

21 F. L. Bernard, L. M. dos Santos, M. B. Schwab, B. B. Polesso, J. F. do Nascimento and S. Einloft, *J. Appl. Polym. Sci.*, 2019, **136**, 47536.

22 Linde, The Linde Group, http://www.linde-engineering.com/.

23 L. Riboldi and O. Bolland, *Energy Procedia*, 2017, **114**, 2390–2400.

24 R. M. Cuéllar-Franca, P. García-Gutiérrez, S. F. R. Taylor, C. Hardacre and A. Azapagic, *Faraday Discuss.*, 2016, **192**, 283–301.

25 J. Sauer, C. Knight, C. Everly and C. Chi, *US*, 20070260089, 2005.

26 S. A. Dharaskar, K. L. Wasewar, M. N. Varma, D. Z. Shende and C. Yoo, *Arabian J. Chem.*, 2016, **9**, 578–587.

27 K. Eller, E. Henkes, R. Rossbacher, H. Höke, K. Eller, E. Henkes, R. Rossbacher and H. Höke, in *Ullmann's Encyclopedia of Industrial Chemistry*, Wiley-VCH Verlag GmbH & Co. KGaA, Weinheim, Germany, 2000.

28 Y. Li, Q. Li, L. Zhi and M. Zhang, *Catal. Lett.*, 2011, **141**, 1635–1642.

29 ISO, ISO 14040 - Environmental management – Life cycle assessment – Principles and framework, http://www.iso.org/iso/catalogue_detail?csnumber=37456.

30 ISO, ISO 14044 - Environmental management – Life cycle assessment – Requirements and guidelines, http://www.iso.org/iso/catalogue_detail?csnumber=38498.

31 Ecoinvent, ecoinvent v3.1, http://www.ecoinvent.org/home.html.

32 M. Rossberg, W. Lendle, G. Pfleiderer, A. Tögel, T. R. Torkelson, K. K. Beutel, M. Rossberg, W. Lendle, G. Pfleiderer, A. Tögel, T. R. Torkelson and K. K. Beutel, in *Ullmann's Encyclopedia of Industrial Chemistry*, Wiley-VCH Verlag GmbH & Co. KGaA, Weinheim, Germany, 2011.

33 F. Su, C. Lu and H.-S. Chen, *Langmuir*, 2011, **27**, 8090–8098.

34 US DoE, APPENDIX B: Carbon Dioxide Capture Technology Sheets Post-Combustion Sorbents, https://www.netl.doe.gov/FileLibrary/Research/Coal/carbon capture/handbook/CO2-Capture-Tech-Update-2013-Post-Combustion-Sorbents.pdf.

35 A. Mehrkesh and A. T. Karunanithi, *ACS Sustainable Chem. Eng.*, 2013, **1**, 448–455.

36 Thinkstep, GaBi LCA Software, https://www.thinkstep.com/software/gabi-lca.

37 Universiteit Leiden Institute of Environmental Sciences (CML), CML-IA Characterisation Factors, https://www.universiteitleiden.nl/en/research/research-output/science/cml-ia-characterisation-factors.

38 S. F. R. Taylor, C. McCrellis, C. McStay, J. Jacquemin, C. Hardacre, M. Mercy, R. G. Bell and N. H. de Leeuw, *J. Solution Chem.*, 2015, **44**, 511–527.

39 K. T. Chue, J. N. Kim, Y. J. Yoo, S. H. Cho and R. T. Yang, *Ind. Eng. Chem. Res.*, 1995, **34**, 591–598.

40 J. Kim, L.-C. Lin, J. A. Swisher, M. Haranczyk and B. Smit, *J. Am. Chem. Soc.*, 2012, **134**, 18940–18943.

41 V. K. Singh and E. Anil Kumar, *Appl. Therm. Eng.*, 2016, **97**, 77–86.

42 P. Bayer, E. Heuer, U. Karl and M. Finkel, *Water Res.*, 2005, **39**, 1719–1728.

43 M. M. Yeganeh, T. Kaghazchi and M. Soleimani, *Chem. Eng. Technol.*, 2006, **29**, 1247–1251.

44 S. Himeno, T. Komatsu and S. Fujita, *J. Chem. Eng. Data*, 2005, **50**, 369–376.

45 Z. Zhang, W. Zhang, X. Chen, Q. Xia and Z. Li, *Sep. Sci. Technol.*, 2010, **45**, 710–719.

46 S. Cavenati, C. A. Grande and A. E. Rodrigues, *J. Chem. Eng. Data*, 2004, **49**, 1095–1101.

47 T. L. Sønderby, K. B. Carlsen, P. L. Fosbol, L. G. Kiorboe and N. von Solms, *Int. J. Greenhouse Gas Control*, 2013, **12**, 181–192.